Proceedings of the 24th UK Conference of the
Association for Computational Mechanics in Engineering
31 March - 01 April 2016, Cardiff University, Cardiff

A MICRO-MECHANICS BASED SOIL-FIBRE COMPOSITE MODEL FOR USE WITH FINITE ELEMENT ANALYSIS

*Thomas Bower[1]**, Anthony Jefferson**[1]**, Peter Cleall**[1] **and Paul Lyons**[2]

[1]School of Engineering, Cardiff University, Queen's buildings, The Parade, Cardiff, CF24 3AA
[2]LUSAS, Forge House, 66 High Street, Kingston Upon Thames, Surrey, KT1 1HN

*BowerTA@cardiff.ac.uk

ABSTRACT

Inclusion of manufactured fibres into a soil has been shown to significantly increase its shear strength and modify its dilative behaviour. The primary mechanism for strength increase is due to the frictional interaction between individual fibres and soil particles. Each fibre resists the movement of soil around it and this has an overall effect of increasing the shear strength. This paper presents the initial development of a micro-mechanics based soil-fibre model which uses concepts from the well-known shear lag model and is extended to include fibre de-bonding. The distribution of fibre orientations is taken into account by use of a distribution function which can be modified according to different soil-fibre preparation techniques. The micro-mechanical model is homogenised using a spherical integration technique and inserted into a single point constitutive driver using the rule of mixtures. The hardening soil model was chosen as a matrix material for this study as it captures the non-linear stress-strain response and failure limit observed in triaxial compression tests. The proposed soil-fibre model is then compared against triaxial compression test data of a well graded sand with differing fibre contents of Loksand fibres and different confining stresses. Preliminary simulations of the experimental tests show promising results.

Key Words: *soil fibre composite; debonding; orientation distribution; constitutive model; triaxial tests*

1. Introduction

Adding fibres to a soil can significantly improve some of its properties. Several studies have shown to increase ultimate shear strength in sands in triaxial compression tests , and a decrease in dilatancy [6, 4, 12]. The strength of the composite is also heavily dependent on the distribution fibre orientations [11] such that the fibres aligned with the direction of the largest extension have the largest effect on the strength, hence the sample preparation method can have some effect on the composite strength [9].

Several soil-fibre models have been developed in recent years; namely by Maher and Gray [10] who used a statistical distribution function to model the variation of fibre orientations. Diambra et al. [6] used a similar basis for their model which also included an empirical debonding function. Diambra and Ibraim [7] improved this model by using shear lag theory [5] as a basis for debonding.

2. Behaviour of a single fibre

The matrix strain ε_{ma} surrounding the fibre drives the composite analysis (Figure 1). Balancing the interface shear forces and the internal tensile forces on an infinitesimal length of fibre gives the well known shear lag equation [5]. Manipulation of the shear lag equation and substitution of the fibre boundary conditions leads to a relationship for the fibre slip.

$$S(x, \varepsilon_{ma}) = \frac{\varepsilon_{ma}}{\beta \cosh(\beta l_f/2)} \sinh(\beta x) \qquad (1)$$

Where β is a material constant relating to the geometry and stiffness of the fibre and soil; it also includes a constant k_s relating the interface slip to the interface shear stress.
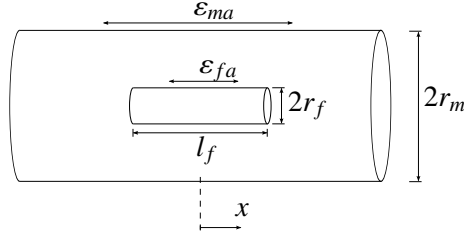
Figure 1: Soil-fibre composite cylinder

$$\sigma_{fa}(x, \varepsilon_{ma}) = \frac{-2k_s \varepsilon_{ma}}{r_f \beta^2 \cosh(\beta l_f / 2)} (\cosh(\beta x) - 1) \tag{2}$$

After extensive loading, the interface will reach a shear stress limit τ_b (Figure 2), this is the debonding shear stress which can be found from the peak tensile load during a fibre pullout test. As the shear stress is always maximum at the fibre ends, debonding occurs first at the ends of the fibre and moves towards the centre with additional loading. The total length of this debonded region is $2l_b$.
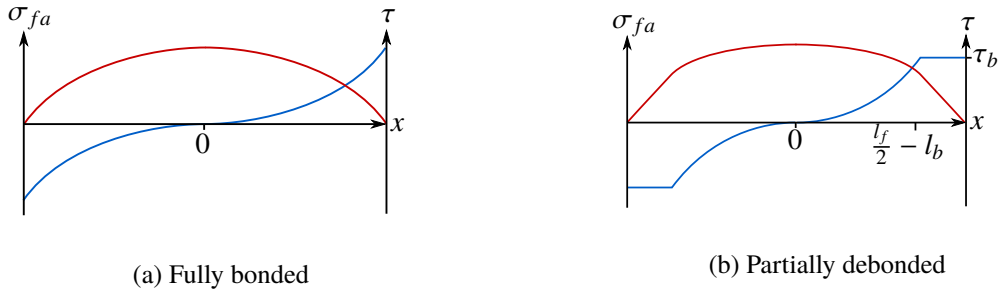

(a) Fully bonded

(b) Partially debonded

Figure 2: Tensile fibre stress σ_{fa} (—) and interface shear stress τ (—) distributions for bonded and partially debonded fibre along the length of the fibre.

Using a similar approach to the fully bonded case, the partially debonded slip relationship is given in Equation (3).

$$S = \begin{cases} \dfrac{\tau_b}{k_s} \dfrac{\sinh(\beta x)}{\sinh(\beta(l_f/2 - l_b))} & \text{if } 0 < x \leq l_f/2 - l_b \\ \dfrac{\tau_b}{k_s} & \text{if } l_f/2 - l_b < x \leq l_f/2 \end{cases} \tag{3}$$

Again, the fibre tensile stress σ_{fa} for the debonding case can be found by substituting the slip relationship in (3) into the shear lag equation and integrating. The stress distribution within the fibre for full and partial bonding can be found in Figure 2.

3. Continuum homogenisation

To analyse the global effect of fibre inclusion, the effects of a single fibre are averaged; taking into account the distribution of orientations and the volume fraction v_f. The distribution of fibres on the horizontal plane is uniform, and the vertical directions are assumed to follow the distribution (4) [11] where θ is the angle from horizontal. The constants $A = 0$, $B = 0.57$, $n = 7$ were determined by comparing with an experimental distribution study [14] for the sand and fibres used in this investigation .

$$\rho_\theta = A + B|\cos^n \theta| \tag{4}$$

The fibre stress relation is then integrated over its length, and over the surface of a sphere using the numerical approach by Bažant and Oh [1] with $n_d = 21$ sampling directions. $\chi(\theta_{id})$ is a transformation vector and w_{id} is a sampling weight.

$$\sigma_f = v_f \sum_{i_d=1}^{n_d} \rho(\theta_{id}) \cdot \chi(\theta_{id})^T \int_0^{l_f/2} \frac{2}{l_f} \sigma_{fa}(x, \varepsilon_{ma}) \, \mathrm{d}x \cdot w_{id} \tag{5}$$

4. The hardening soil model

The soil model chosen to be used alongside the fibre model is the hardening soil model [2, 13]. The model extends the hyperbolic soil model from a hypo-elastic one to an elasto-plastic one. The hardening soil model makes use of multiple yield surfaces, however, this study uses only a modified version of the hardening shear surface. The original yield surface is shown in Equation (6), its modification (which is to be presented in future work) focusses on the robustness of the model, as well as developing a total strain formulation suitable for use in commercial finite element analysis software.

$$f = \frac{q_a}{E_{50}} \frac{q}{q_a - q} - \frac{2q}{E_{ur}} - \gamma_p \tag{6}$$

An explanation of the terms used here may be found in [2]. The plastic potential function is the Drucker-Prager cone [8] with a constant dilatancy angle.

5. Comparison with experimental results and discussion

The unreinforced sand exhibits a non-linear stress / strain relationship during triaxial loading with an upper limit to the available shear stress. This is reflected well in the predicted results whereby soil failure is reached at approximately 5% axial strain (Figure 3a). The strength is under-predicted by 10% and is most likely due to the chosen material parameters. The soil undergoes an initial compression then dilates from 2.2% axial strain. The predicted model also follows this trend but to a different dilating gradient. This is almost certainly due to the simplified dilatancy rule used in the hardening soil model and the lack of a cap surface.

Adding fibres to the soil appears to increase the shear strength indefinitely. The predictions capture the rate of strength increase well. Increased fibre content also reduces dilatancy in the experimental results; this is reflected in the prediction however the limitation with the dilatancy rule does not allow the model to give accurate results here. Also, none of the experimental results presented so far show and significant debonding characteristics, therefore it is not possible to determine the effectiveness of the debonding relationship described in Equation (3).

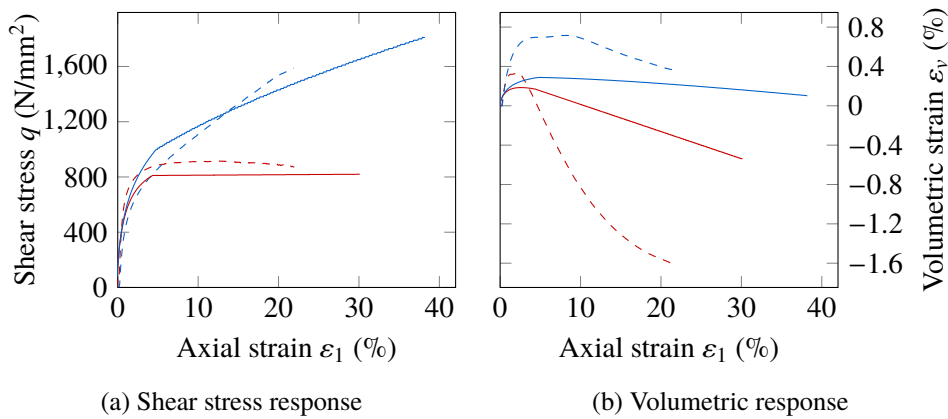(a) Shear stress response   (b) Volumetric response

Figure 3: Triaxial test experimental results (dashed) and predicted (solid); for unreinforced sand (red) and with 0.3% fibre content by volume (blue); experimental results by Chatzopoulos [3]

6. Conclusions

The soil-fibre composite model described here performs to some degree as expected from experimental results. However, limitations in the underlying soil model may be dominating over any shortcomings in the fibre model. Therefore, further work will focus on completing the re-formulation of the hardening soil model and testing of the soil-fibre model under different conditions.

Acknowledgements

References

[1] Z. P. Bažant and B. H Oh. Efficient numerical integration on the surface of a sphere. *ZAMM - Journal of Applied Mathematics and Mechanics*, 66(1), 37-49, 1986.

[2] T. Benz. Small-strain stiffness of soils and its numerical consequences, PhD. Thesis, Univ. Stuttgart, Inst. f. Geotechnik, 2007.

[3] S. Chatzopoulos. Soil reinforced with discrete polypropylene fibers, MSc. Thesis, Cardiff University, 2015.

[4] N. C. Consoli, P. D. M. Prietto, and L. A. Ulbrich. Influence of fiber and cement addition on behaviour of sandy soil. *Journal of Geotechnical and Geoenvironmental Engineering*, 124(12), 1211-1214, 1998.

[5] H. L. Cox. The elasticity and strength of paper and other fibrous materials. *British Journal of Applied Physics*, 3, 72-79, 1952.

[6] A. Diambra E. Ibraim, D. Muir Wood and A. R. Russel. Fibre-reinforced sands: Experiments and modelling. *Geotextiles and geomembranes*, 28(3), 238-250, 2010.

[7] A. Diambra and E. Ibraim. Fibre-reinforced sand: interaction at the fibre and grain scale. *Géotechnique*, 65, 296-308, 2015.

[8] D. C. Drucker, W. Prager and H. T. Greenberg. Extended limit design theorems for coninuous media, *Quarterly of applied mathematics*, 1952.

[9] E. Ibraim, A. Diambra, A.R. Russel and D. Muir Wood. Assessment of laboratory sample preparation for fibre reinforced sands. *Geotextiles and Geomembranes*, 34, 69-79, 2012.

[10] M. H. Maher, and D. H. Gray. Static response of sands reinforced with randomly distributed fibres. *Journal of Geotechnical Engineering*, 116(11), 1661-1677, 2012.

[11] R. L. Michalowski and J. Čermák. Strength anisotropy of fibre-reinforced sand. *Computers and Geotechnics*, 29(4), 279-299, 2002.

[12] R. L. Michalowski and J. Čermák. Triaxial compression of sand reinforced with fibers. *Journal of Geotechnical and Geoenvironmental Engineering*, 129(2), 125-136, 2003.

[13] T. Schanz, P. A Vermeer and P. G. Bonnier. The hardening soil model: formulation and verification. *Beyond 2000 in computational geotechnics*, 281-296, 1999.

[14] Z. Wang. Fibre reinforced sand: from sample preparation to triaxial tests and orientation investigation, MSc. Thesis, Cardiff University, 2015.